

Designing Coulombic Contact Interactions between Polarizable Particles through Asymmetry

Yanyu Duan[†] and Zecheng Gan^{*,†,‡}

[†]*Thrust of Advanced Materials, and Guangzhou Municipal Key Laboratory of Materials Informatics, The Hong Kong University of Science and Technology (Guangzhou), Guangzhou 511453, China.*

[‡]*Department of Mathematics, The Hong Kong University of Science and Technology, Hong Kong SAR, China*

E-mail: zechenggan@ust.hk

Abstract

Polarizable particle systems, including charged colloids, polarizable ions, biomolecular assemblies, and soft nanomaterials, can exhibit contact electrostatic interactions that depart strongly from Coulomb behavior when dielectric mismatch and geometric singularities amplify polarization effects. Here we use charged dielectric spheres as a model system and show that these polarization contributions can be canceled by jointly tuning size, charge, and dielectric asymmetries. By extending a recently developed image-charge formula to contacting dielectric spheres, we derive analytical conditions under which the contact interaction reduces to the bare Coulomb form. Accurate two-sphere calculations validate the resulting contact design rules with relative errors below 3%. Strikingly, many-body molecular dynamics simulations reveal that systems satisfying these two-body rules self-assemble into structures that closely match

their pure Coulomb references. These results establish asymmetry as a route for turning electrostatic complexity into Coulombic simplicity at contact, with implications for controlled self-assembly and materials design.

Keywords

dielectric spheres, polarization, image charges, self-assembly

Introduction

Electrostatic interactions are often treated as bare Coulomb interactions when charged particles approach one another, but this approximation can fail at contact in polarizable systems. Charged colloids, polarizable ions, biomolecular assemblies, and soft nanomaterials commonly contain dielectric interfaces, and the induced charges at these interfaces can reshape short-range forces that control aggregation, crystallization, and self-assembly.¹⁻⁵ A minimal model that isolates this mechanism consists of charged dielectric spheres immersed in a homogeneous medium whose permittivity differs from that of the particles.⁶ Despite its simple geometry, this model captures the essential contact-scale challenge: dielectric mismatch and geometric singularities can amplify polarization contributions until the interaction departs strongly from the Coulomb limit.

These departures are not small corrections. Recent studies have shown that conductor-like particles, whose dielectric permittivity is higher than that of the surrounding medium, can exhibit short-range “like-charge attraction”, especially under size or charge asymmetry.⁷⁻⁹ Conversely, insulator-like particles can show “opposite-charge repulsion” under related conditions.¹⁰ Such effects make contact electrostatics difficult to predict and difficult to use as a design variable: the same nominal Coulomb interaction can be strengthened, weakened, or even effectively reversed by polarization. A central question is therefore whether polarization at contact must be treated only as a complication, or whether it can be deliberately canceled

by tailoring size, charge, and dielectric asymmetries between the particles.

The electrostatic contact problem has a long history, beginning with Maxwell’s analysis of conducting spheres and later work on weak singularities in conductor polarization energy.^{11,12} For dielectric particles, Qin and co-workers derived induced-charge equations in bispherical coordinates to describe the contact energy of identical dielectric spheres and later extended the analysis to clusters of contacting dielectrics.^{13,14} More broadly, substantial progress has been made in computing and understanding polarization in dielectric sphere systems, including bispherical-coordinate treatments of two-sphere contact,¹⁵ polarizable ion models,¹⁶ multiple-scattering formalisms,^{17–19} boundary integral equations,^{20–22} image-charge methods,^{23,24} and the method of moments.²⁵ However, these advances do not yet provide a simple materials design framework for contacting dielectric spheres with simultaneous size, charge, and dielectric asymmetries.

In this Letter, we show that asymmetry can be used to program Coulombic contact interactions between polarizable particles. We first revisit a recently developed image-charge formula for polarizable spheres⁸ and extend it to charged dielectric spheres in contact. The resulting analytical expression separates the bare Coulomb interaction from polarization contributions controlled by size, charge, and dielectric asymmetries, allowing us to derive cancellation conditions under which the contact energy reduces to the Coulomb form. We validate these contact design rules against accurate hybrid-method simulations,²⁶ with all relative errors below 3%; many-body molecular dynamics simulations further show that designed polarizable systems self-assemble into structures that closely match their pure Coulomb references. Together, this framework turns size, charge, and dielectric asymmetries from apparent sources of electrostatic complexity into design parameters for recovering Coulombic simplicity in polarizable particle assemblies, with implications for controlled self-assembly and soft materials design.

Theory

The design objective is to make the electrostatic contact energy between two polarizable spheres recover the bare Coulomb energy, $E_{\text{ele}} = E_{\text{Coul}}$, even when the spheres have dielectric mismatch with the surrounding medium. To reach this objective analytically, the theory must separate the contact energy into a direct Coulomb term and a polarization correction whose sign and magnitude can be tuned by material and geometric asymmetry. We obtain this separation by extending a recently developed compact image-charge formula for dielectric spheres⁸ to the contact geometry.

We first recall the single-sphere building block. Consider a point charge Q interacting with a neutral dielectric sphere of radius a and dielectric constant ϵ_{in} , both immersed in a homogeneous medium with permittivity ϵ_{out} , as depicted in Fig.1(a). According to the

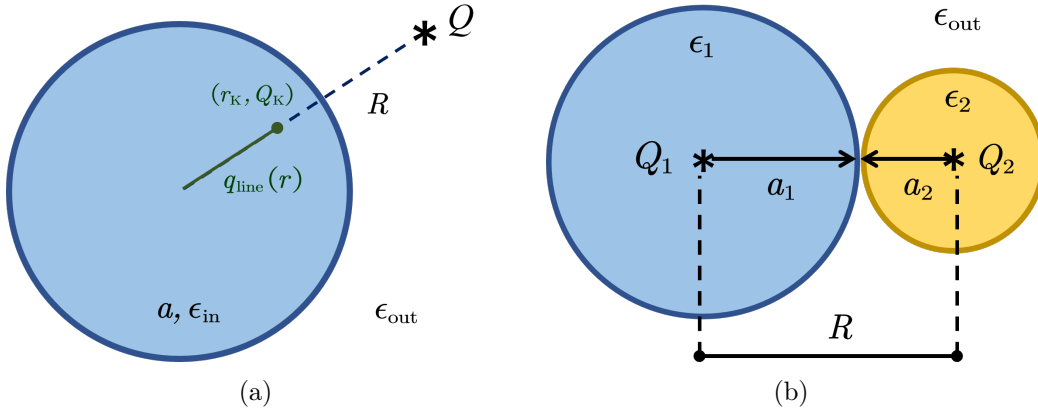


Figure 1: Schematics of the dielectric sphere model. (a) A point charge Q interacts with a neutral dielectric sphere of radius a and dielectric constant ϵ_{in} at separation R . According to Neumann's image principle, the polarization potential is generated by a Kelvin image charge Q_K at r_K and a line image charge density $q_{\text{line}}(r)$ distributed along the green line connecting the Kelvin point and the sphere center. (b) A pair of charged dielectric spheres in contact, with radii (a_1, a_2) , dielectric constants (ϵ_1, ϵ_2) , and central charges (Q_1, Q_2) . Both systems are immersed in a medium with permittivity ϵ_{out} .

classical *Neumann image principle*,^{27,28} the polarization potential outside the sphere can be represented by a Kelvin image charge $Q_K = -\frac{Qka}{R}$ located at $r_K = \frac{a^2}{R}$ and a Neumann image line with charge density $q_{\text{line}}(r) = \frac{Qka}{a} \left(\frac{r_K}{r}\right)^{1-g}$ distributed from the sphere center to

the Kelvin point. Here the dimensionless dielectric contrast is $k = \frac{\epsilon_{\text{in}} - \epsilon_{\text{out}}}{\epsilon_{\text{in}} + \epsilon_{\text{out}}}$, and $g = \frac{1}{1 + \frac{\epsilon_{\text{in}}}{\epsilon_{\text{out}}}}$. The polarization energy E_{pol} for the single-sphere system is then

$$E_{\text{pol}} = \frac{1}{2} \frac{Q}{4\pi\epsilon_0\epsilon_{\text{out}}} \left[\frac{Q_{\text{K}}}{R - r_{\text{K}}} + \int_0^{r_{\text{K}}} \frac{q_{\text{line}}(r)}{R - r} dr \right], \quad (1)$$

where ϵ_0 is the vacuum permittivity, and the extra prefactor $1/2$ accounts for the fictitious nature of image charges. In the perfect-conductor limit, i.e., $\epsilon_{\text{in}} \rightarrow +\infty$, the line charge density degenerates to a point charge at the sphere center and Eq. (1) reduces to the classical image formula for a spherical conductor.²⁹ For a finite dielectric constant ϵ_{in} , however, direct use of the image-line integral is inconvenient because the line charge is singular at the sphere center ($r = 0$). Although tailored discretization schemes enable this representation in Monte Carlo (MC) and molecular dynamics (MD) simulations,^{21,30,31} the integral form does not directly lead to a simple analytical design rule for canceling the contact polarization correction.

By defining the dimensionless separation variable $t = \frac{a}{R}$, Eq. (1) can be equivalently written as⁸

$$E_{\text{pol}} = \frac{1}{2} \frac{Q}{4\pi\epsilon_0\epsilon_{\text{out}}R} \left[-\frac{Qkt}{1 - t^2} + \frac{Qktg}{t^{2g}} B_{t^2}(g, 0) \right], \quad (2)$$

where $B_{t^2}(g, 0)$ is the incomplete beta function.³² Using the series expansion for $B_{t^2}(g, 0)$,³³

$$B_{t^2}(g, 0) = t^{2g} \sum_{n=0}^{\infty} \frac{t^{2n}}{n + g}, \quad (3)$$

and substituting $g = \frac{1-k}{2}$, Eq. (2) can be simplified as

$$E_{\text{pol}} = -\frac{1}{2} \frac{Q^2kt}{4\pi\epsilon_0\epsilon_{\text{out}}R} \left[\frac{1}{1 - t^2} - (1 - k) \sum_{n=0}^{\infty} \frac{t^{2n}}{2n + 1 - k} \right]. \quad (4)$$

Equation (4) is mathematically equivalent to Neumann's image principle, but it replaces the singular image-line integral in Eq. (1) with a simple series. This series form is the key step

that makes the contact-cancellation problem analytically tractable.

We now consider two dielectric spheres in contact, as shown in Fig.1(b). The spheres may have different radii (a_1, a_2) , dielectric constants (ϵ_1, ϵ_2) , and central charges (Q_1, Q_2) , with center-to-center distance $R = a_1 + a_2$. Applying Eq. (4) to each sphere, and treating the central charge in the other sphere as the external source charge, gives the first-reflection contact energy

$$E_{\text{ele}} = \frac{Q_1 Q_2}{4\pi\epsilon_0\epsilon_{\text{out}}(a_1 + a_2)} \left\{ 1 - \frac{k_2 t_2}{2} \frac{Q_1}{Q_2} \left[\frac{1}{1 - t_2^2} - (1 - k_2) \sum_{n=0}^{\infty} \frac{t_2^{2n}}{2n + 1 - k_2} \right] - \frac{k_1 t_1}{2} \frac{Q_2}{Q_1} \left[\frac{1}{1 - t_1^2} - (1 - k_1) \sum_{n=0}^{\infty} \frac{t_1^{2n}}{2n + 1 - k_1} \right] \right\}, \quad (5)$$

where $k_1 = \frac{\epsilon_1 - \epsilon_{\text{out}}}{\epsilon_1 + \epsilon_{\text{out}}}$, $k_2 = \frac{\epsilon_2 - \epsilon_{\text{out}}}{\epsilon_2 + \epsilon_{\text{out}}}$, $t_1 = \frac{a_1}{a_1 + a_2}$, $t_2 = \frac{a_2}{a_1 + a_2}$, and clearly $t_1 + t_2 \equiv 1$. Equation (5) provides the desired decomposition: the prefactor is the bare Coulomb interaction, $E_{\text{Coul}} = \frac{Q_1 Q_2}{4\pi\epsilon_0\epsilon_{\text{out}}(a_1 + a_2)}$, and the bracket contains one plus a polarization correction. Equivalently, $E_{\text{ele}}/E_{\text{Coul}} = 1 + \Phi$, where Φ is controlled only by the dielectric contrasts $k_{1,2}$, the contact size ratios $t_{1,2}$, and the charge ratio Q_1/Q_2 . The contact-design condition is therefore simply $\Phi = 0$: the polarization terms generated by the two spheres must cancel each other. This formulation turns size, charge, and dielectric asymmetries into explicit control parameters rather than uncontrolled sources of deviation from Coulomb behavior.

Equation (5) is a leading-order expression for the contact energy because it truncates the mutual image-reflection series at the first reflection. Higher-order reflections give a more complete two-sphere polarization energy and have been used in numerical simulation studies.^{23,34,35} Here the purpose of Eq. (5) is not to serve as a high-precision electrostatic solver, but to provide an analytical route to the cancellation conditions used for materials design. We benchmark this approximation against a highly accurate numerical method:³⁶ the contact-energy benchmarks reported in Table S1 of the *Supporting Information* (SI) show relative errors all within 5%.

Role of dielectric asymmetry

To expose the cancellation mechanism in its simplest form, we first remove charge and size asymmetry and isolate dielectric asymmetry alone; the isolated effects of charge and size asymmetry are discussed in the SI. Here we set $Q_1 = Q_2 = Q$ and $a_1 = a_2 = a$, so that $t_1 = t_2 = \frac{1}{2}$. In this case, the contact energy Eq. (5) becomes

$$E_{\text{ele}} = \frac{Q^2}{4\pi\epsilon_0\epsilon_{\text{out}}(2a)} \left[1 - \frac{k_1 + k_2}{3} + \frac{k_1(1 - k_1)}{4} \sum_{n=0}^{\infty} \frac{4^{-n}}{2n + 1 - k_1} + \frac{k_2(1 - k_2)}{4} \sum_{n=0}^{\infty} \frac{4^{-n}}{2n + 1 - k_2} \right]. \quad (6)$$

Equivalently, the normalized contact energy can be written as

$$\frac{E_{\text{ele}}}{E_{\text{Coul}}} = 1 + \psi(k_1) + \psi(k_2), \quad \psi(k) = -\frac{k}{3} + \frac{k(1 - k)}{4} \sum_{n=0}^{\infty} \frac{4^{-n}}{2n + 1 - k}. \quad (7)$$

This decomposition makes the role of dielectric asymmetry transparent. The function $\psi(k)$ is zero at $k = 0$, positive for insulator-like particles ($-1 < k < 0$), and negative for conductor-like particles ($0 < k < 1$). Thus two particles with dielectric contrasts of the same sign push the contact energy to the same side of the Coulomb value and cannot cancel each other's polarization contributions. Cancellation requires the two contributions in Eq. (7) to have opposite signs, which means that one sphere must be conductor-like and the other insulator-like.

In Fig. 2, we plot the contact energy (normalized by the pure Coulomb energy E_{Coul}) versus k_1 , with varying $k_2 \in (-1, 1)$. For fixed k_2 , the contact energy decreases monotonically as k_1 (or ϵ_1) increases, consistent with the monotonic decrease of $\psi(k_1)$. When k_1 and k_2 have the same sign ($k_1 k_2 > 0$), the contact energy is weakened relative to the Coulomb energy for two conductor-like spheres ($k_1 > 0, k_2 > 0$) and enhanced for two insulator-like spheres ($k_1 < 0, k_2 < 0$). When $k_1 k_2 < 0$, the two polarization corrections compete, so the contact

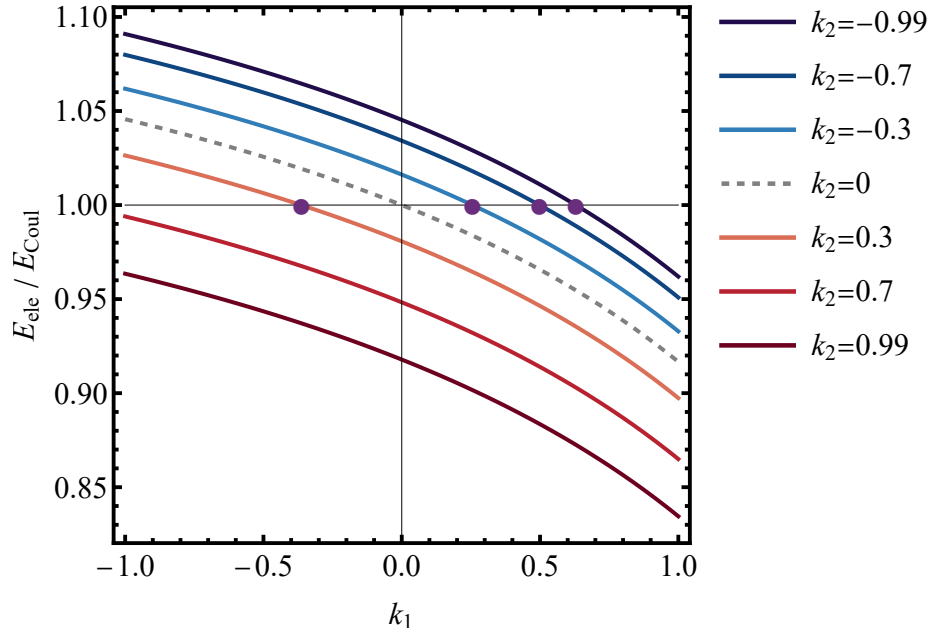


Figure 2: Influence of dielectric asymmetry ($k_1 \neq k_2$) on the contact energy. The normalized contact energy ($E_{\text{ele}}/E_{\text{Coul}}$) is plotted versus k_1 for different k_2 . Filled circles indicate nontrivial (k_1, k_2) pairs for which the polarization correction vanishes.

energy can lie above, below, or exactly at the Coulomb limit depending on their relative magnitudes. The filled circles in Fig. 2 mark the nontrivial solutions of $\psi(k_1) + \psi(k_2) = 0$, where the contact energy returns to E_{Coul} even though both spheres remain polarizable. Dielectric asymmetry alone therefore already reveals the basic design principle: the contact energy can recover the bare Coulomb value even with finite dielectric mismatch, provided that the two spheres generate polarization corrections of opposite sign. For equal charges and equal sizes, however, this condition defines only a narrow cancellation curve on the (k_1, k_2) plane. We next show how further introducing charge or size asymmetry expands this curve into a broader design space.

Design rules for Coulombic contact interactions

The cancellation condition identified above can be generalized by returning to Eq. (5) and allowing additional asymmetry to tune the two polarization terms. We now derive explicit

design rules for recovering $E_{\text{ele}} = E_{\text{Coul}}$ by simultaneously adjusting dielectric asymmetry with either charge or size asymmetry. For clarity, we consider two experimentally transparent scenarios: (a) two equal-sized spheres with both charge and dielectric asymmetries; and (b) two unequal-sized spheres with dielectric asymmetry and equal charge magnitudes.

The design rule is obtained by setting the polarization correction in Eq. (5) to zero. To keep the cancellation conditions transparent, we define the single-sphere contact polarization response

$$\mathcal{P}(k, t) = kt \left[\frac{1}{1-t^2} - (1-k) \sum_{n=0}^{\infty} \frac{t^{2n}}{2n+1-k} \right].$$

This response depends on both the dielectric contrast k and the contact size ratio t ; its sign distinguishes conductor-like and insulator-like particles. For scenario (a), $t_1 = t_2 = 1/2$, and charge asymmetry changes only the relative weights of the two dielectric polarization terms. The charge ratio Q_1/Q_2 and dielectric contrasts k_1 and k_2 must therefore satisfy

$$\left(\frac{Q_1}{Q_2}\right)^2 \mathcal{P}\left(k_2, \frac{1}{2}\right) + \mathcal{P}\left(k_1, \frac{1}{2}\right) = 0. \quad (8)$$

For a fixed charge ratio, Eq. (8) gives the dielectric-contrast pairs (k_1, k_2) for which the two weighted polarization corrections cancel. Changing $|Q_1/Q_2|$ therefore shifts the cancellation curve in the (k_1, k_2) plane. Because only $(Q_1/Q_2)^2$ appears, the contact-energy design rule is independent of whether the two particles are like charged or oppositely charged. We therefore plot the feasible sets in Fig. 3(a) using $Q_1/Q_2 > 0$ without loss of generality. The series defining \mathcal{P} is rapidly convergent; truncating at $n_{\text{max}} = 10$ is sufficient for all curves shown here.

For scenario (b), we set equal charge magnitudes and use size asymmetry to tune the two polarization responses. Sphere 1 contributes through the contact ratio t_1 , whereas sphere 2 contributes through $t_2 = 1 - t_1$. The cancellation condition is therefore

$$\mathcal{P}(k_2, 1 - t_1) + \mathcal{P}(k_1, t_1) = 0. \quad (9)$$

For a fixed t_1 , Eq. (9) gives the dielectric-contrast pairs (k_1, k_2) that recover the Coulomb contact interaction. Changing t_1 changes the relative weights of the two single-sphere responses, so each size ratio produces a different cancellation curve, as shown in Fig. 4(a).

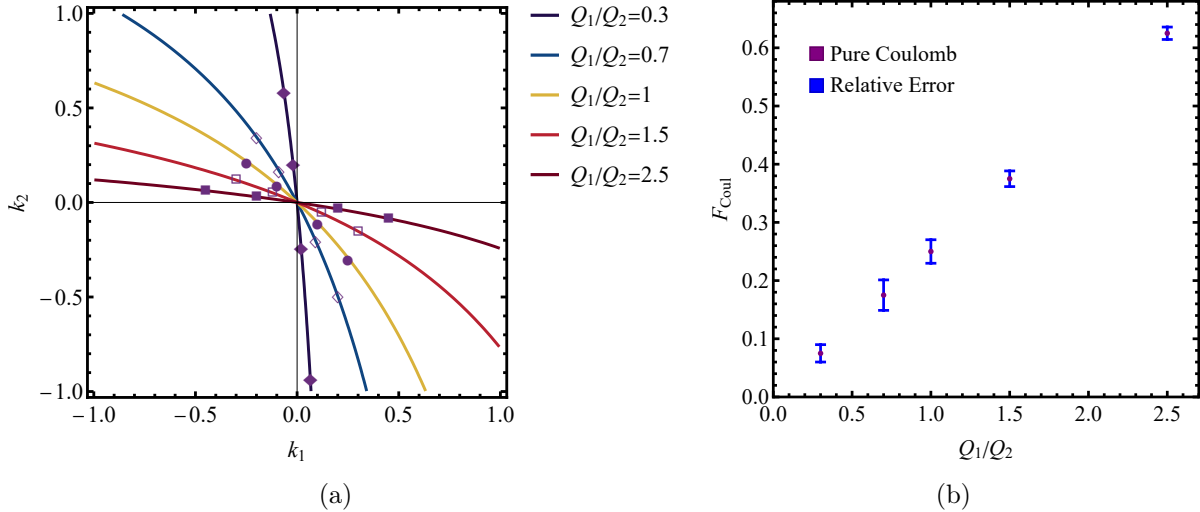


Figure 3: (a) Predicted design rules for recovering the pure Coulomb contact interaction by jointly tuning charge and dielectric asymmetries. Feasible sets of dielectric contrast pairs (k_1, k_2) are plotted for different charge asymmetries Q_1/Q_2 . Markers indicate selected validation data points. (b) Numerical validation by comparing the simulated electrostatic contact force for the designed parameters with the pure Coulomb force F_{Coul} ; error bars are calculated from the validation data marked in Fig. 3(a), with details listed in Table S2 of the SI.

Figures 3(a) and 4(a) show that, in both scenarios, all feasible dielectric-contrast pairs (k_1, k_2) lie in the second and fourth quadrants. This confirms the necessary condition anticipated from Eq. (7): canceling the contact polarization correction requires $k_1 k_2 < 0$, so one sphere must be conductor-like and the other insulator-like. When only dielectric asymmetry is present ($Q_1/Q_2 = 1$ in Fig. 3(a) and $t_1 = 0.5$ in Fig. 4(a)), the feasible set reduces to the narrow cancellation curve identified in Fig. 2. Introducing charge or size asymmetry reweights the two competing polarization corrections and expands this curve into a broader family of dielectric design rules while preserving the sign requirement $k_1 k_2 < 0$.

To validate the design rules predicted by Eqs. (8) and (9), we selected representative parameter sets labeled in Figs. 3(a) and 4(a) and computed the corresponding interaction

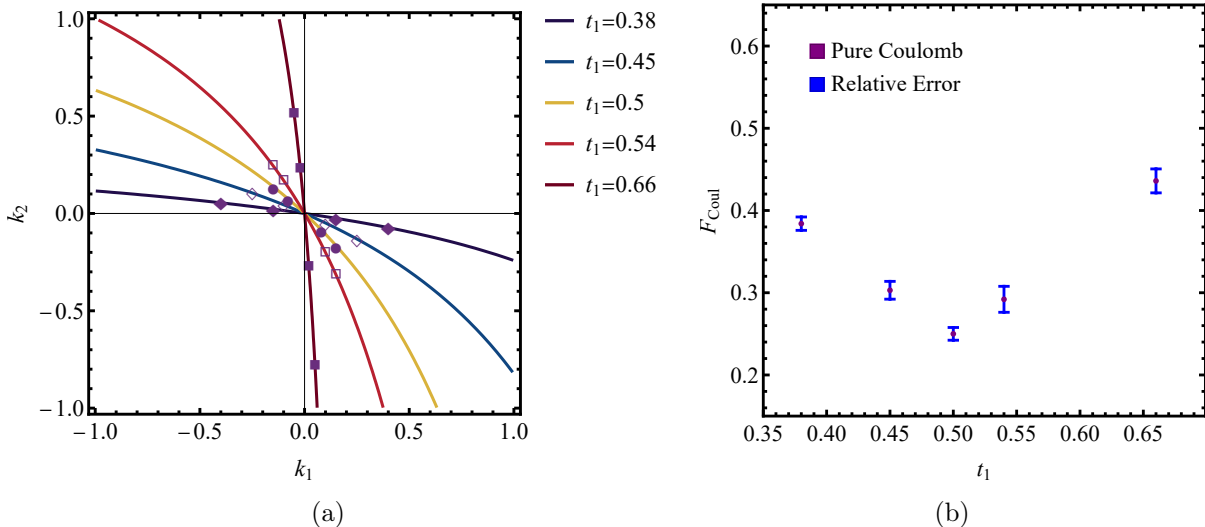


Figure 4: (a) Predicted design rules for recovering the pure Coulomb contact interaction by jointly tuning size and dielectric asymmetries. Feasible sets of dielectric contrast pairs (k_1, k_2) are plotted for different size asymmetries t_1 . Markers indicate selected validation data points. (b) Numerical validation by comparing the simulated electrostatic contact force for the designed parameters with the pure Coulomb force F_{Coul} ; error bars are calculated from the validation data marked in Fig. 4(a), with details listed in Table S3 of the SI.

forces with an accurate numerical method.²⁶ Because Eqs. (8) and (9) are derived from the contact energy, we further test whether the same designed parameters also reproduce the Coulomb force at contact. The computed electrostatic forces are compared with the pure Coulomb force F_{Coul} in Figs. 3(b) and 4(b) for scenarios (a) and (b), respectively; each error bar is obtained from four parameter sets with fixed charge or size asymmetry. For both scenarios, the designed polarizable pairs recover the pure Coulomb force with relative errors below 3% for all data sets (Tables S2 and S3 of the SI), demonstrating that the analytical cancellation conditions are quantitatively predictive.

Self-assembly with designed Coulomb interactions

We next explore whether the two-body contact rules remain predictive in many-body self-assembly. This is not guaranteed a priori, because polarization in a many-particle assembly is a many-body response rather than a simple sum of isolated pair corrections. Nevertheless,

if the designed parameters suppress the dominant contact-scale polarization contribution, the resulting short-range structure should closely follow that of a pure Coulomb reference in this strongly coupled assembly regime. To test this expectation, we performed MD simulations using the Hybrid Method²⁶ for designed polarizable systems and their pure Coulomb references. Each system contains 200 charged dielectric spheres at a total volume fraction of 3%. The temperature is controlled by a Langevin thermostat, and the coupling strength is fixed at $\lambda = |E_{\text{Coul}}|/(k_{\text{B}}T) = 100$, where $E_{\text{Coul}} = \frac{Q_1 Q_2}{4\pi\epsilon_0\epsilon_{\text{out}}(a_1+a_2)}$ is the direct Coulomb interaction between two spheres in contact.

For the equal-sized test, the system contains 100 spheres of each type with opposite charges $Q_1/Q_2 = -1$ and equal radii $a_1/a_2 = 1$. The pure Coulomb reference uses $\epsilon_1 = \epsilon_2 = 1$, whereas the designed polarizable system uses $\epsilon_1 = 1.35294$ and $\epsilon_2 = 0.71782$, corresponding to a nontrivial dielectric-asymmetry design point satisfying Eq. (8). For the unequal-sized test, the system again contains 100 spheres of each type with $Q_1/Q_2 = -1$, but the radii satisfy $a_1/a_2 = 0.613$. The pure Coulomb reference uses $\epsilon_1 = \epsilon_2 = 1$, whereas the designed polarizable system uses $\epsilon_1 = 2.33333$ and $\epsilon_2 = 0.86446$, corresponding to a size-dielectric design point satisfying Eq. (9).

The radial distribution functions (RDFs) $\Gamma(R_{s-s})$ for the equal-sized and unequal-sized systems are shown in Figs. 5(a) and 5(b), respectively. In both tests, the designed polarizable systems closely overlap with the pure Coulomb references, including the contact peak and the subsequent coordination shells. The snapshots in the insets show similar self-assembled aggregate morphologies. Strikingly, this agreement persists beyond the calibrated two-sphere contact force: a cancellation condition derived for an isolated contact also recovers, for the assembled systems tested here, the many-body structural correlations of the corresponding pure Coulomb references. This connection between contact-level cancellation and assembly-level structure shows that the Coulombic contact design rule developed here can be carried beyond isolated particle pairs.

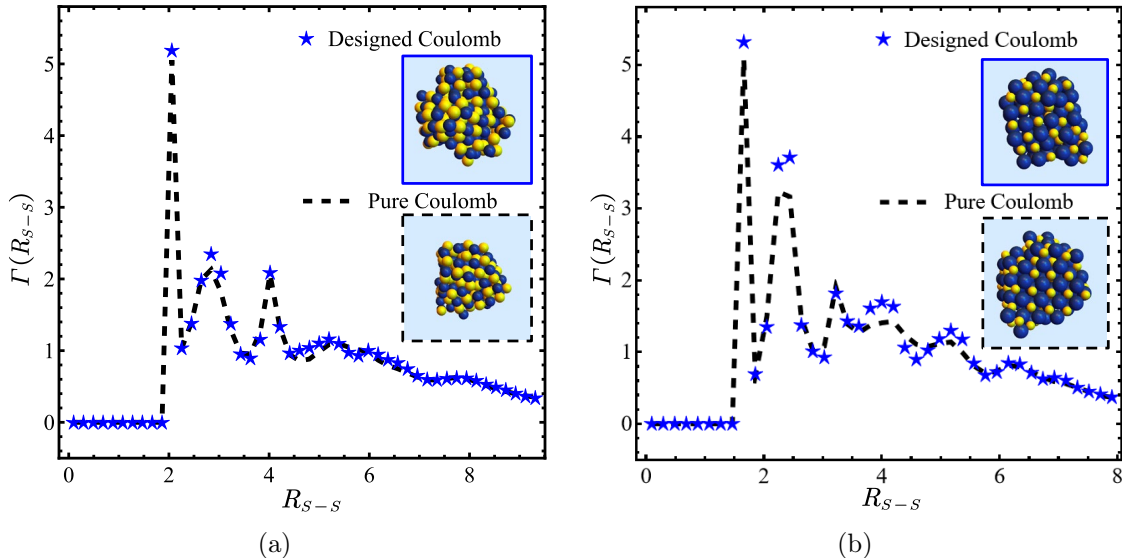


Figure 5: Many-body validation of designed Coulombic contact interactions. Radial distribution functions for (a) equal-sized and (b) unequal-sized oppositely charged spheres ($N = 200$) under designed conditions [Eqs. (8) and (9)] (stars) closely match the pure Coulomb references (dashed), showing that the pair-level cancellation design also preserves the many-body structural correlations in these tested assemblies. R_{s-s} : center-to-center distance between spheres with opposite charges. Insets: typical snapshots.

Conclusion

This work establishes asymmetry as a design variable for recovering Coulombic contact interactions between polarizable particles. By extending a compact image-charge formula to contacting dielectric spheres, we separated the bare Coulomb interaction from the leading polarization correction controlled by size, charge, and dielectric asymmetries. This decomposition yields analytical cancellation conditions under which the contact energy returns to the Coulomb value even though both particles remain dielectric mismatched with the surrounding medium.

The resulting design rules show that cancellation requires opposite-sign dielectric contrasts, $k_1 k_2 < 0$, so that one sphere contributes a conductor-like correction and the other an insulator-like correction. Charge or size asymmetry then reweights these competing contributions and expands the narrow dielectric-asymmetry cancellation curve into a broader

family of feasible material parameters. Accurate two-sphere calculations validate the designed contact forces with relative errors below 3%, while many-body simulations show that the tested designed systems reproduce the RDFs and aggregate morphologies of their pure Coulomb references. Thus, a contact-level cancellation rule can remain predictive for structural correlations in assembled polarizable systems, rather than serving only as an isolated two-particle result.

The present framework is formulated for charged dielectric spheres in a homogeneous medium, so mobile ions and charge-regulating surfaces are outside its scope. It therefore excludes ionic screening in electrolytes,^{37–39} electrolyte-mediated attractions and anti-Coulomb effects,^{40–44} charge regulation,^{45–47} and continuum Poisson–Boltzmann electrostatics,^{48,49} all of which could alter the cancellation conditions. Extending this design framework to screened electrostatics and dense assemblies with multiple simultaneous contacts^{50–52} would further test the generality of asymmetry-guided Coulombic contact design in polarizable soft materials.

Acknowledgement

The authors would like to acknowledge financial support from the Natural Science Foundation of China (Grant No. 12201146) and the Natural Science Foundation of Guangdong Province (Grant No. 2023A1515012197). Both authors would like to thank Professor Ho-Kei Chan for insightful discussions.

Supporting Information Available

Contact energy validation

This section validates the leading-order contact-energy expression used to generate the analytical design rules in the main text. The system parameters, calculated contact energies,

benchmark reference values, and relative errors are listed in Table 1.

Analysis for contact energy: the role of asymmetries

Two-sphere systems with charge asymmetry

We first isolate charge asymmetry by setting the dielectric constants and radii to be symmetric, i.e., $\epsilon_1 = \epsilon_2 = \epsilon_{\text{in}}$ ($k_1 = k_2 = k$), and $a_1 = a_2 = a$ ($t_1 = t_2 = t = \frac{a}{2a} = \frac{1}{2}$). Therefore, the contact energy expression in the main text reduces to

$$E_{\text{ele}} = \frac{Q_1 Q_2}{4\pi\epsilon_0\epsilon_{\text{out}}(2a)} \left\{ 1 - \frac{k}{4} \left(\frac{Q_1}{Q_2} + \frac{Q_2}{Q_1} \right) \left[\frac{4}{3} - (1-k) \sum_{n=0}^{\infty} \frac{4^{-n}}{2n+1-k} \right] \right\}. \quad (10)$$

Figs. 6(a) and 6(b) illustrate the impact of charge asymmetry on the contact energy of like-charged and oppositely charged spheres, respectively. In each scenario, we plot the contact energy normalized by the pure Coulomb energy, $E_{\text{ele}}/E_{\text{Coul}}$, versus $(Q_1/Q_2 + Q_2/Q_1)$, with varying dielectric contrast values $k \in (-1, 1)$. The dimensionless parameter $(Q_1/Q_2 + Q_2/Q_1)$, which appears in Eq. (10), characterizes the strength of charge asymmetry: for like-charged spheres, it reaches its minimum value of 2 when $Q_1 = Q_2$; for oppositely charged spheres, its magnitude increases as the charge asymmetry increases.

Figs. 6(a) and 6(b) show that, in the absence of dielectric contrast ($k = 0$), the contact energy is equal to the pure Coulomb energy. When $k \neq 0$, the contact energy deviates from the Coulomb value as the charge asymmetry or dielectric mismatch increases. For conductor-like spheres ($k > 0$), the normalized contact energy is lower than the Coulomb value, indicating weakened like-charge repulsion or enhanced opposite-charge attraction. For insulator-like spheres ($k < 0$), the normalized contact energy is higher than the Coulomb value, indicating enhanced like-charge repulsion or weakened opposite-charge attraction. These trends are consistent with earlier studies of polarization-induced like-charge attraction and opposite-charge repulsion.^{8,10}

Table 1: Contact-energy validation for a pair of identical dielectric spheres with charges ($Q_1 = Q_2 = Q$), dielectric constants ($\epsilon_1 = \epsilon_2 = \epsilon_{\text{in}}$), and radii ($a_1 = a_2 = a$), suspended in a homogeneous medium with permittivity ϵ_{out} . The dielectric contrast is defined as $k = (\epsilon_{\text{in}} - \epsilon_{\text{out}})/(\epsilon_{\text{in}} + \epsilon_{\text{out}})$. Both E_{Ref} and E_{ele} are contact energies: E_{Ref} denotes reference values from the literature,¹³ and E_{ele} denotes the leading-order analytical result used in this work. Both energies are expressed in units of $\frac{Q^2}{4\pi\epsilon_0\epsilon_{\text{out}}a}$.

k	E_{Ref}	E_{ele}	$\text{Err}\left(\left \frac{E_{\text{ele}}-E_{\text{Ref}}}{E_{\text{Ref}}}\right \right)$
-0.960	0.563	0.544	3.375%
-0.871	0.556	0.541	2.698%
-0.775	0.549	0.537	2.186%
-0.678	0.542	0.533	1.661%
-0.581	0.535	0.529	1.121%
-0.488	0.529	0.525	0.756%
-0.391	0.523	0.521	0.382%
-0.295	0.516	0.516	0
-0.196	0.511	0.511	0
-0.099	0.505	0.505	0
0	0.5	0.5	0
0.042	0.496	0.497	0.202%
0.188	0.487	0.488	0.205%
0.315	0.480	0.480	0
0.476	0.471	0.468	0.637%
0.639	0.461	0.454	1.518%
0.784	0.452	0.440	2.655%
0.960	0.442	0.421	4.751%

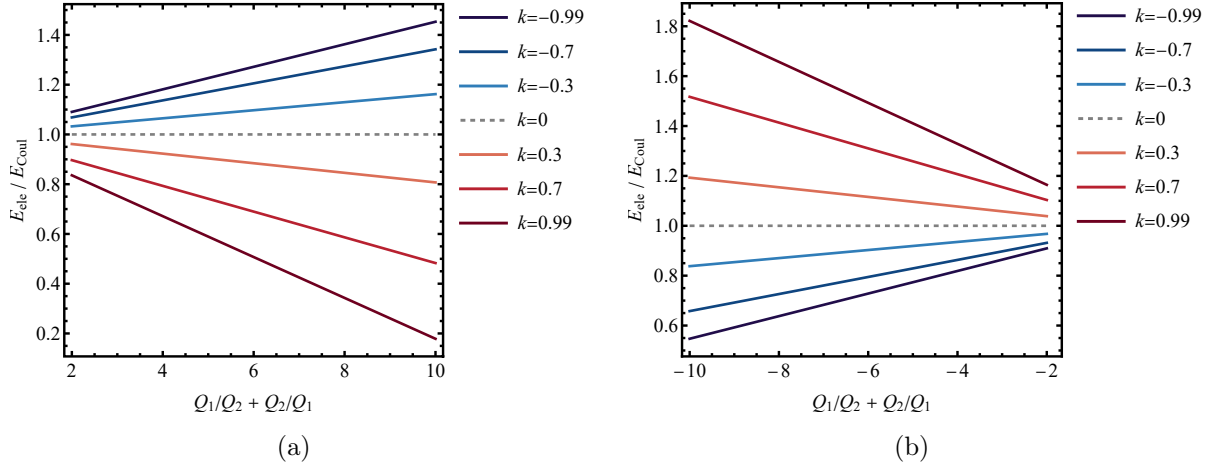


Figure 6: Influence of charge asymmetry $\left(\frac{Q_1}{Q_2} + \frac{Q_2}{Q_1}\right)$ on the contact energy of two-sphere systems. (a) Like-charged spheres ($Q_1Q_2 > 0$) and (b) oppositely charged spheres ($Q_1Q_2 < 0$). In each scenario, the normalized contact energy $E_{\text{ele}}/E_{\text{Coul}}$ is plotted versus $(Q_1/Q_2 + Q_2/Q_1)$ for different dielectric contrasts k .

Two-sphere systems with size asymmetry

We next isolate size asymmetry by considering a pair of spheres with radii a_1 and a_2 , while setting $Q_1 = Q_2 = Q$ and $k_1 = k_2 = k$. For contacting spheres, the contact ratios satisfy $t_1 + t_2 = 1$, where $t_1 = a_1/(a_1 + a_2)$ and $t_2 = a_2/(a_1 + a_2)$. Hence, by substituting $t_2 = 1 - t_1$, the contact energy expression in the main text becomes

$$E_{\text{ele}} = \frac{Q^2}{4\pi\epsilon_0\epsilon_{\text{out}}(a_1 + a_2)} \left\{ 1 - \frac{kt_1}{2} \left[\frac{1}{1-t_1^2} - (1-k) \sum_{n=0}^{\infty} \frac{t_1^{2n}}{2n+1-k} \right] - \frac{k(1-t_1)}{2} \left[\frac{1}{t_1(2-t_1)} - (1-k) \sum_{n=0}^{\infty} \frac{(1-t_1)^{2n}}{2n+1-k} \right] \right\}. \quad (11)$$

In Fig. 7, we plot the contact energy (normalized by the pure Coulomb energy E_{Coul}) versus t_1 , with varying dielectric contrast $k \in (-1, 1)$. Fig. 7 shows that, when the two spheres are equal sized ($t_1 = t_2 = 0.5$), the contact energy reaches an extremum for each dielectric contrast k . As the size asymmetry increases (t_1 approaches either 0 or 1), the contact energy deviates increasingly from the pure Coulomb energy E_{Coul} . Under extreme dielectric contrast and size asymmetry, the contact energy can become several times larger

than the pure Coulomb value or even reverse sign because of strong polarization. As in Fig. 6, conductor-like spheres ($k > 0$) weaken the normalized contact energy, whereas insulator-like spheres ($k < 0$) enhance it.

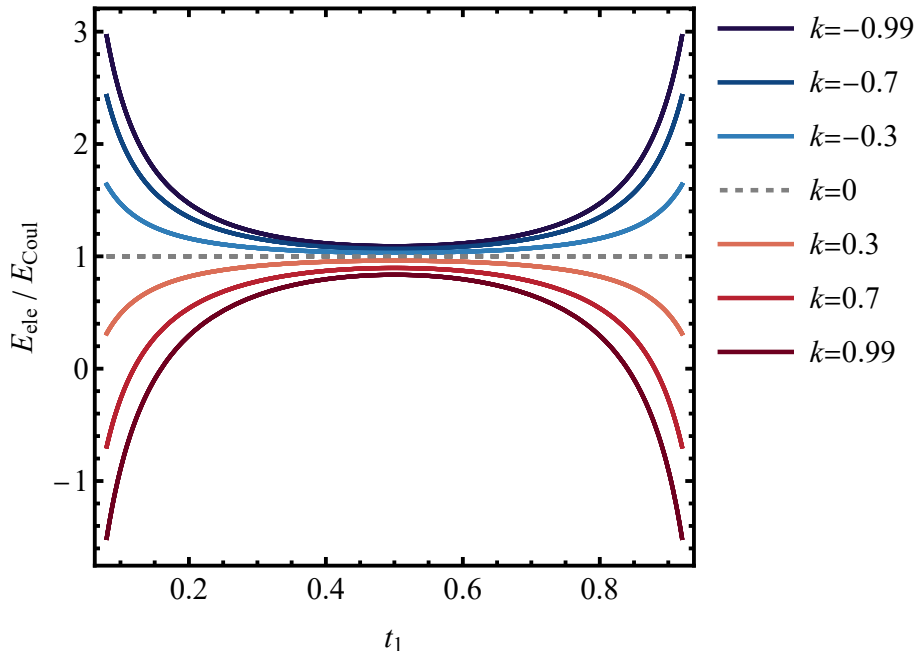


Figure 7: Influence of size asymmetry ($t_1 \neq t_2$) on the contact energy of two-sphere systems. The normalized contact energy $E_{\text{ele}}/E_{\text{Coul}}$ is plotted versus t_1 for different dielectric contrasts $k \in (-1, 1)$.

Validation of the pure Coulomb contact force

Tables 2 and 3 document contact-force validation for representative parameter sets predicted by the analytical design rules and marked in the main-text figures. Table 2 collects the validation data for two-sphere systems with charge and dielectric asymmetries, whereas Table 3 collects the data for systems with size and dielectric asymmetries.

Table 2: Contact-force validation for two equal-sized dielectric spheres in vacuum ($\epsilon_{\text{out}} = 1$). In the simulations, $Q_2 = 1\mu C$ and $a_1 = a_2 = a = 1\mu m$, so the force is reported in units of $\frac{1}{4\pi\epsilon_0} \frac{[C]^2}{[m]^2}$. F_{Coul} and F_{Simul} denote the pure Coulomb force and the force calculated using the Hybrid Method,²⁶ respectively.

$\frac{Q_1}{Q_2}$	k_1	k_2	ϵ_1	ϵ_2	Q_2	F_{Coul}	F_{Simul}	Err $\left(\frac{\sqrt{\frac{\sum_{i=1}^4 (F_{\text{Coul}} - F_{\text{Simul}}^i)^2}{4}}}{ F_{\text{Coul}} } \right)$
0.3	0.065	-0.932	1.139	0.040	1	0.075	0.073	1.493%
	0.02	-0.239	1.041	0.614	1		0.075	
	-0.065	0.587	0.878	3.843	1		0.074	
	-0.02	0.208	0.961	1.525	1		0.075	
0.7	0.09	-0.199	1.198	0.668	1	0.175	0.174	2.617%
	0.2	-0.495	1.5	0.338	1		0.168	
	-0.09	0.170	0.835	1.410	1		0.178	
	-0.2	0.347	0.667	2.063	1		0.170	
1	0.25	-0.292	1.667	0.548	1	0.25	0.242	2.020%
	0.1	-0.106	1.222	0.808	1		0.249	
	-0.25	0.218	0.6	1.558	1		0.244	
	-0.1	0.095	0.818	1.210	1		0.249	
1.5	0.12	-0.056	1.273	0.894	1	0.375	0.374	1.347%
	0.3	-0.153	1.857	0.735	1		0.367	
	-0.12	0.051	0.786	1.107	1		0.374	
	-0.3	0.119	0.538	1.270	1		0.369	
2.5	0.45	-0.085	2.626	0.843	1	0.625	0.614	1.067%
	0.2	-0.034	1.5	0.934	1		0.623	
	-0.45	0.063	0.379	1.134	1		0.618	
	-0.2	0.030	0.667	1.062	1		0.623	

References

- (1) Levin, Y. Electrostatic correlations: from plasma to biology. *Rep. Prog. Phys* **2002**, *65*, 1577.

Table 3: Contact-force validation for two unequal-sized dielectric spheres in vacuum ($\epsilon_{\text{out}} = 1$). In the simulations, $Q_1 = Q_2 = 1\mu C$, and a_1 and a_2 are measured in units of μm , so the force is reported in units of $\frac{1}{4\pi\epsilon_0} \frac{[C]^2}{[m]^2}$. F_{Coul} and F_{Simul} denote the pure Coulomb force and the force calculated using the Hybrid Method,²⁶ respectively.

t_1	t_2	a_1	a_2	k_1	k_2	ϵ_1	ϵ_2	F_{Coul}	F_{Simul}	Err $\left(\frac{\sqrt{\frac{\sum_{i=1}^4 (F_{\text{Coul}} - F_{\text{Simul}}^i)^2}{4}}}{ F_{\text{Coul}} } \right)$
0.38	0.62	0.613	1	0.4	-0.073	2.333	0.864	0.384	0.383	0.813%
				0.15	-0.025	1.353	0.951		0.385	
				-0.4	0.055	0.429	1.116		0.378	
				-0.15	0.022	0.739	1.045		0.383	
0.45	0.55	0.818	1	0.25	-0.131	1.667	0.768	0.303	0.299	1.082%
				0.1	-0.049	1.222	0.907		0.302	
				-0.25	0.106	0.6	1.237		0.298	
				-0.1	0.045	0.818	1.094		0.302	
0.5	0.5	1	1	0.15	-0.164	1.353	0.718	0.25	0.247	0.775%
				0.08	-0.084	1.174	0.845		0.249	
				-0.15	0.138	0.739	1.320		0.248	
				-0.08	0.076	0.852	1.165		0.249	
0.54	0.46	1	0.852	0.15	-0.314	1.353	0.522	0.292	0.285	1.579%
				0.1	-0.200	1.222	0.667		0.288	
				-0.15	0.245	0.739	1.649		0.288	
				-0.1	0.170	0.818	1.410		0.290	
0.66	0.34	1	0.515	0.05	-0.782	1.105	0.122	0.436	0.424	1.455%
				0.02	-0.271	1.041	0.574		0.432	
				-0.05	0.513	0.905	3.107		0.436	
				-0.02	0.229	0.961	1.594		0.437	

(2) French, R. H.; Parsegian, V. A.; Podgornik, R.; Rajter, R. F.; Jagota, A.; Luo, J.; Asthagiri, D.; Chaudhury, M. K.; Chiang, Y.-m.; Granick, S.; others Long range interactions in nanoscale science. *Rev. Mod. Phys* **2010**, *82*, 1887–1944.

- (3) Walker, D. A.; Kowalczyk, B.; de La Cruz, M. O.; Grzybowski, B. A. Electrostatics at the nanoscale. *Nanoscale* **2011**, *3*, 1316–1344.
- (4) Leunissen, M. E.; Christova, C. G.; Hynninen, A.-P.; Royall, C. P.; Campbell, A. I.; Imhof, A.; Dijkstra, M.; Van Roij, R.; Van Blaaderen, A. Ionic colloidal crystals of oppositely charged particles. *Nature* **2005**, *437*, 235–240.
- (5) Kewalramani, S.; Guerrero-García, G. I.; Moreau, L. M.; Zwanikken, J. W.; Mirkin, C. A.; Olvera de la Cruz, M.; Bedzyk, M. J. Electrolyte-mediated assembly of charged nanoparticles. *ACS Cent. Sci.* **2016**, *2*, 219–224.
- (6) Barros, K.; Luijten, E. Dielectric effects in the self-assembly of binary colloidal aggregates. *Phys. Rev. Lett.* **2014**, *113*, 017801.
- (7) Besley, E. Recent developments in the methods and applications of electrostatic theory. *Acc. Chem. Res.* **2023**, *56*, 2267–2277.
- (8) Duan, Y.; Gan, Z. Quantitative theory for critical conditions of like-charge attraction between polarizable spheres. *J. Chem. Theory Comput.* **2025**, *21*, 2822–2828.
- (9) Gorman, M.; Ruan, X.; Ni, R. Electrostatic interactions between rough dielectric particles. *Phys. Rev. E* **2024**, *109*, 034902.
- (10) Duan, Y.; Gan, Z.; Chan, H.-K. Mechanisms of electrostatic interactions between two charged dielectric spheres inside a polarizable medium: An effective-dipole analysis. *Soft Matter* **2025**, *21*, 1860–1872.
- (11) Maxwell, J. C. *A treatise on electricity and magnetism*; Clarendon press, 1873; Vol. 1.
- (12) Lekner, J. Electrostatics of two charged conducting spheres. *Proc. R. Soc. A* **2012**, *468*, 2829–2848.
- (13) Lian, H.; Qin, J. Polarization energy of two charged dielectric spheres in close contact. *Mol. Syst. Des. Eng.* **2018**, *3*, 197–203.

- (14) Lian, H.; Qin, J. Exact polarization energy for clusters of contacting dielectrics. *Soft Matter* **2022**, *18*, 6411–6418.
- (15) Chan, H.-K.; Lindgren, E. B.; Stace, A. J.; Bichoutskaia, E. A General Geometric Representation of Sphere-Sphere Interactions. *Frontiers in Quantum Methods and Applications in Chemistry and Physics: Selected Proceedings of QSCP-XVIII* (Paraty, Brazil, December, 2013). 2015; pp 29–36.
- (16) Chan, H.-K. A theory for like-charge attraction of polarizable ions. *J. Electrostat.* **2020**, *105*, 103435.
- (17) Freed, K. F. Perturbative many-body expansion for electrostatic energy and field for system of polarizable charged spherical ions in a dielectric medium. *J. Chem. Phys.* **2014**, *141*, 034115.
- (18) Qin, J.; Li, J.; Lee, V.; Jaeger, H.; de Pablo, J. J.; Freed, K. F. A theory of interactions between polarizable dielectric spheres. *J. Colloid Interface Sci.* **2016**, *469*, 237–241.
- (19) Qin, J. Charge polarization near dielectric interfaces and the multiple-scattering formalism. *Soft Matter* **2019**, *15*, 2125–2134.
- (20) Barros, K.; Sinkovits, D.; Luijten, E. Efficient and accurate simulation of dynamic dielectric objects. *J. Chem. Phys.* **2014**, *140*, 064903.
- (21) Gan, Z.; Wu, H.; Barros, K.; Xu, Z.; Luijten, E. Comparison of efficient techniques for the simulation of dielectric objects in electrolytes. *J. Comput. Phys.* **2015**, *291*, 317–333.
- (22) Lindgren, E. B.; Stace, A. J.; Polack, E.; Maday, Y.; Stamm, B.; Besley, E. An integral equation approach to calculate electrostatic interactions in many-body dielectric systems. *J. Comput. Phys.* **2018**, *371*, 712–731.

- (23) Xu, Z. Electrostatic interaction in the presence of dielectric interfaces and polarization-induced like-charge attraction. *Phys. Rev. E* **2013**, *87*, 013307.
- (24) Wang, R.; Wang, Z.-G. Effects of image charges on double layer structure and forces. *J. Chem. Phys.* **2013**, *139*, 124702.
- (25) Bichoutskaia, E.; Boatwright, A. L.; Khachatourian, A.; Stace, A. J. Electrostatic analysis of the interactions between charged particles of dielectric materials. *J. Chem. Phys.* **2010**, *133*, 024105.
- (26) Gan, Z.; Wang, Z.; Jiang, S.; Xu, Z.; Luijten, E. Efficient dynamic simulations of charged dielectric colloids through a novel hybrid method. *J. Chem. Phys.* **2019**, *151*, 024112.
- (27) Neumann, C. *Hydrodynamische untersuchungen: nebst einem Anhang über die Probleme der Elektrostatik und der magnetischen Induction*; BG Teubner, 1883.
- (28) Lindell, I. *URSI Review of Radio Science 1990-1992*; Clarendon Press, 1993; pp 107–126.
- (29) Jackson, J. D. *Classical electrodynamics*; John Wiley & Sons, 2021.
- (30) Cai, W.; Deng, S.; Jacobs, D. Extending the fast multipole method to charges inside or outside a dielectric sphere. *J. Comput. Phys.* **2007**, *223*, 846–864.
- (31) Gan, Z.; Xu, Z. Multiple-image treatment of induced charges in Monte Carlo simulations of electrolytes near a spherical dielectric interface. *Phys. Rev. E* **2011**, *84*, 016705.
- (32) Arfken, G. B.; Weber, H. J.; Harris, F. E. *Mathematical methods for physicists: a comprehensive guide*; Academic press, 2011.
- (33) Pearson, K.; others *Tables of the incomplete beta-function*; Cambridge University Press Cambridge, 1968; Vol. 1.

- (34) Li, X.; Li, C.; Gao, X.; Huang, D. Like-charge attraction between two identical dielectric spheres in a uniform electric field: A theoretical study via a multiple-image method and an effective-dipole approach. *J. Mater. Chem. A* **2024**, *12*, 6896–6905.
- (35) Li, X.; Li, C.; Chen, X.; Wang, Z.; Min, S.; Huang, D. Electrostatic interaction of neutral particles on a dielectric substrate: A theoretical study via a multiple-image method and an effective-dipole approach. *Phys. Rev. E* **2025**, *111*, 045505.
- (36) Gan, Z.; Jiang, S.; Luijten, E.; Xu, Z. A hybrid method for systems of closely spaced dielectric spheres and ions. *SIAM J. Sci. Comput.* **2016**, *38*, B375–B395.
- (37) Lee, H. M.; Kim, Y. W.; Go, E. M.; Revadekar, C.; Choi, K. H.; Cho, Y.; Kwak, S. K.; Park, B. J. Direct measurements of the colloidal Debye force. *Nat. Commun.* **2023**, *14*, 3838.
- (38) Yuan, J.; Antila, H. S.; Luijten, E. Particle–particle particle–mesh algorithm for electrolytes between charged dielectric interfaces. *J. Chem. Phys.* **2021**, *154*, 094115.
- (39) Becker, M. R.; Netz, R. R.; Loche, P.; Bonthuis, D. J.; Mouhanna, D.; Berthoumieux, H. Dielectric properties of aqueous electrolytes at the nanoscale. *Phys. Rev. Lett.* **2025**, *134*, 158001.
- (40) Wang, S.; Walker-Gibbons, R.; Watkins, B.; Flynn, M.; Krishnan, M. A charge-dependent long-ranged force drives tailored assembly of matter in solution. *Nat. Nanotechnol.* **2024**, *19*, 485–493.
- (41) Allahyarov, E.; D’amico, I.; Löwen, H. Attraction between like-charged macroions by Coulomb depletion. *Phys. Rev. Lett.* **1998**, *81*, 1334.
- (42) Wills, A.; Mannino, A.; Losada, I.; Mayo, S. G.; Soler, J. M.; Fernández-Serra, M. Anti-Coulomb ion-ion interactions: A theoretical and computational study. *Phys. Rev. Res.* **2024**, *6*, 033095.

- (43) Dos Santos, A. P.; Levin, Y. Like-charge attraction between metal nanoparticles in a 1:1 electrolyte solution. *Phys. Rev. Lett.* **2019**, *122*, 248005.
- (44) Zhang, R.; Shklovskii, B. Long-range polarization attraction between two different like-charged macroions. *Phys. Rev. E* **2005**, *72*, 021405.
- (45) Messina, R.; Holm, C.; Kremer, K. Strong attraction between charged spheres due to metastable ionized states. *Phys. Rev. Lett.* **2000**, *85*, 872.
- (46) Yuan, J.; Takae, K.; Tanaka, H. Impact of charge regulation on self-assembly of zwitterionic nanoparticles. *Phys. Rev. Lett.* **2022**, *128*, 158001.
- (47) López-Flores, L.; Olvera de la Cruz, M. Charge regulation effects on colloidal mixture nanoparticles. *J. Chem. Phys.* **2025**, *163*, 034303.
- (48) Budkov, Y. A.; Kolesnikov, A. L. Modified Poisson–Boltzmann equations and macroscopic forces in inhomogeneous ionic fluids. *J. Stat. Mech.: Theory Exp.* **2022**, *2022*, 053205.
- (49) Budkov, Y. A.; Kalikin, N. N.; Brandyshev, P. E. Surface tension of aqueous electrolyte solutions. A thermomechanical approach. *J. Chem. Phys.* **2024**, *160*, 164701.
- (50) Nitzke, I.; Lishchuk, S. V.; Vrabec, J. Long-range corrections for molecular simulations with three-body interactions. *J. Chem. Theory Comput.* **2024**, *21*, 1–4.
- (51) Avis, H.; Lindgren, E. B.; Stamm, B.; Besley, E.; Stace, A. J. The Accommodation of Excess Charge in Binary Particle Lattices: A Many-Body Electrostatic Study. *J. Phys. Chem. B* **2025**, *129*, 9789–9794.
- (52) Lindgren, E. B.; Avis, H.; Miller, A.; Stamm, B.; Besley, E.; Stace, A. J. The significance of multipole interactions for the stability of regular structures composed from charged particles. *J. Colloid Interface Sci.* **2024**, *663*, 458–466.